

CVOCSemRPL: Class-Variance Optimized Clustering, Semantic Information Injection and Restricted Pseudo Labeling based Improved Semi-Supervised Few-Shot Learning

Rhythm Baghel*, Souvik Maji*, Pratik Mazumder*,[©]
 Indian Institute of Technology Jodhpur, India

b22cs042@iitj.ac.in, b22cs089@iitj.ac.in, pratikm@iitj.ac.in

Abstract

Few-shot learning has been extensively explored to address problems where the amount of labeled samples is very limited for some classes. In the semi-supervised few-shot learning setting, substantial quantities of unlabeled samples are available. Such unlabeled samples are generally cheaper to obtain and can be used to improve the few-shot learning performance of the model. Some of the recent methods for this setting rely on clustering to generate pseudo-labels for the unlabeled samples. Since the quality of the representation learned by the model heavily influences the effectiveness of clustering, this might also lead to incorrect labeling of the unlabeled samples and consequently lead to a drop in the few-shot learning performance. We propose an approach for semi-supervised few-shot learning that performs a class-variance optimized clustering in order to improve the effectiveness of clustering the labeled and unlabeled samples in this setting. It also optimizes the clustering-based pseudo-labeling process using a restricted pseudo-labeling approach and performs semantic information injection in order to improve the semi-supervised few-shot learning performance of the model. We experimentally demonstrate that our proposed approach significantly outperforms recent state-of-the-art methods on the benchmark datasets.

always be available in sufficient quantities for the required tasks and labeling data itself is a costly and time-consuming process. Therefore, researchers have been looking at few-shot learning as a solution to this problem. In this paper, we address the semi-supervised few-shot learning problem.

The few-shot learning setting involves training a model to learn new classes using an extremely small number of labeled samples of these classes. This is a difficult task for deep learning models. In order to address this problem, few-shot learning approaches use transfer learning from a set of base classes that have sufficient labeled samples. Few-shot learning approaches use the base class example to learn a good representation, which is then used to extract good features from the few samples of the few-shot classes. As a result, the quality of representation plays a vital role in the few-shot learning performance.

Even with extensive research in few-shot learning [1, 27, 24, 3, 12], the performance of such methods is still limited due to the extremely limited availability of labeled samples. However, even though the amount of labeled samples available for the few-shot classes is very limited, we may still have access to large quantities of unlabeled samples since these are relatively easier to obtain as compared to labeled samples. The unlabeled samples can be used to improve the performance on the few-shot classes. This modified setting constitutes the semi-supervised few-shot learning setting.

Researchers have proposed multiple approaches to address the semi-supervised few-shot learning problem. Many such methods predict pseudo-labels for the unlabeled samples and utilize them to improve the performance on the few-shot classes. Recent methods have used techniques like clustering to assign pseudo-labels to unlabeled samples [22, 17]. Clustering relies heavily on the quality of representation learned by the network, especially on the base classes. Good quality representation ensures that newly observed images, even from unseen classes, are far away from images of other classes and close to images from the same class in the representation space. Clustering based on features extracted

1. Introduction

Deep learning has made inroads into numerous types and varieties of real-world tasks, and deep learning models have had a significant success in outperforming humans in several tasks. In order to solve many real-world complex tasks, deep learning models have become deeper and more complex with millions or billions of parameters. In order to train models with so many parameters, we generally need to use large volumes of labeled data. However, labeled data may not

* All the authors contributed equally.

© Corresponding author

by networks with low-quality representation learning would lead to imperfect clustering and consequently lead to incorrect pseudo-labels getting assigned to the unlabeled samples. Such incorrectly labeled samples would severely restrict the performance of the few-shot learning methods and, in the worst case, even harm the model performance.

In this work, we propose a novel approach to better optimize a semi-supervised few-shot learning model that counteracts the above problems using an optimized clustering-based approach. Specifically, we use a class variance optimized clustering (CVOC) process to cluster labeled images of a class and use a semantic injection network to refine the cluster centers by incorporating semantic information. We use the refined cluster centers to perform restricted pseudo-labeling of the unlabeled samples and incorporate all labeled samples to make predictions for the query samples. The details of our proposed approach have been provided in Sec. 4.

We perform experiments on multiple semi-supervised few-shot learning benchmark datasets and demonstrate that our proposed approach significantly outperforms the compared approaches. We also perform ablation experiments to demonstrate the contributions of the different components of our approach.

The key contributions of this paper are as follows:

1. We propose a novel semi-supervised few-shot learning approach that outperforms the recent methods in this setting, as shown in Tables 1, 2, 3.
2. We experimentally demonstrate how incorporating semantic features of classes and managing the intra-class and inter-class distance losses helps to further improve the performance of the model, as shown in Table 4.

2. Related Works

2.1. Few-shot Image Classification

Few-shot image classification algorithms seek to establish a training and updating methodology appropriate for few-shot contexts [10, 33]. Researchers have explored different varieties of approaches to address the few-shot learning task. A very simple but effective work was proposed in [25] that utilized an average feature prototype of the classes with very few samples and performed predictions by identifying the nearest prototype. There are multiple transfer-learning based methodologies that pre-train the model using extensive data from the base classes and subsequently modify the pre-trained model for the few-shot learning job of recognizing novel categories. Another FSL method TADAM [19] adapts the features of the few-shot class images using the few support images available for such classes. The work in [9] improves upon prototypical network using importance-weighting strategy for the different support samples of a class and makes the prototypes more informative.

Meta-learning methods learn to quickly adapt to new classes using very few samples and these methods involve training a model at a specific level as well as at an abstract level, referred to as learning to learn. [34]. Researchers have proposed various meta-learning-based few-shot learning approaches such as [2], which was one of the first use of meta learning in few-shot learning and its objective was to achieve a good initialization of the parameters such that it could quickly adapt to a new class using very few labeled samples. Methods like [15, 20] attempted to optimize the model update mechanisms for faster and efficient meta-learning. The authors in [26] re-weight useful features to ensure that they have a higher influence on the output using channel-wise attention and a meta-level drop-out technique.

In this paper, similar to existing few-shot learning and semi-supervised few-shot learning methods, we utilize a pre-training step for the visual feature extractor on the base classes which helps it learn to extract good features for the novel class images during testing.

2.2. Pseudo-labeling based Semi-supervised Few-shot Methods

Since unlabeled samples are generally easier to obtain than labeled samples, researchers have been working on a modified few-shot learning setting, i.e., the semi-supervised few-shot learning setting. Many such semi-supervised few-shot learning methods try to improve the model performance by assigning pseudo-labels to samples that are not annotated with any labels. Once the pseudo-labels have been obtained for some of the unlabeled images, such methods generally consider these samples as labeled samples and use them for the few-shot classification task. A common problem faced by all such method is that in case some of the pseudo labels are incorrect, that severely restricts the performance of the model. Some methods utilize label propagation to generate pseudo-labels [18] while some methods focus on pretraining for better pseudo-label prediction [34]. The work in [11] carefully optimizes low-capacity classifier to identify good quality pseudo labels and iteratively refines them.

Previous methods such as Wu et al. [31] prioritization of informative samples and Sun et al.'s [14] selective sampling of high-confidence labels are notable, yet they treat each sample independently and miss out on broader relational context. Additionally, Huang et al.'s pseudo-loss confidence metric (PLCM) [7] attempts to unify pseudo-labeled data in a single metric space but also does not consider these inter-sample relationships, which limits its effectiveness.

Huang et al.'s Poisson Transfer Network (PTN) [6] further addresses these limitations by incorporating some relational understanding between labeled and unlabeled samples. However, PTN lacks the capacity to effectively mine inter- and intra-class relationships and to prevent the inclusion of noisy labels. Wang et al.'s Instance Credibility Inference (ICI) [30]

attempts to rank pseudo-labels based on credibility and sparsity, yet it neglects the issue of low-quality pseudo-labels, which can introduce noise into the clustering process.

Cluster-FSL [17] employs a multi-factor clustering (MFC) strategy, which synthesizes various information sources from labeled data to produce both soft and hard pseudo-labels. However, we experimentally observed that the pseudo-labeling strategy employed by it, led to most of the unlabeled images becoming eligible for pseudo-labeling. Cluster-FSL’s limitations are rooted in its inadequate handling of inter-class and intra-class relationships, which restricts its ability to differentiate effectively between distinct classes and to capture subtle variations within individual classes. This gap in modeling these relationships affects the method’s precision and depth, particularly for complex datasets where finer distinctions are crucial. This led to unlabeled samples with incorrect pseudo-labels being considered as labeled samples and consequently limiting the performance of the model.

In this work, we propose to mitigate these limitations through a class-variance optimized clustering (CVOC) approach and, which aligns the embedding space according to both inter- and intra-class relationships using targeted loss functions and also by using a firefly algorithm. The proposed approach also incorporates semantic features to further improve the clustering process. Further, the proposed approach also performs restricted pseudo-labeling and allocates pseudo-labels exclusively to unlabeled samples with low entropy predictions, reducing the possibility of noisy pseudo-labels affecting the model performance.

3. Problem Setting

In the vanilla few-shot learning setting, the data contains two types of classes, namely the base classes C_b and the novel/few-shot classes C_f . The base classes have a sufficient number of training samples available, while the novel classes have very few training samples. There is no overlap between the base and novel classes. The dataset is divided into the train set D_{tr} , the validation set D_{va} , and the test set D_{tt} . The train set D_{tr} only contains samples from the base classes while the validation D_{va} and test D_{tt} sets contain samples from the novel classes. There is also no overlap between the classes in the validation set and the test set. Data is provided to the network in the form of N -way K -shot episodes, where N refers to the number of classes in the episode, and K refers to the number of support/training samples from each of these classes. The support set can be denoted as $S = (x_i^s, y_i^s)_{i=0}^{N \times K}$. The episode also contains T randomly selected query/test samples from each of these classes on which the model can be evaluated. The query set can be denoted as $Q = (x_i^q, y_i^q)_{i=0}^{N \times T}$. The episodes from the train set contain a support set S and a query set Q from N randomly selected classes from among the classes in the

train set. Similarly, the episodes from the test set contain a support set S and a query set Q from N randomly selected classes from among the classes in the test set. In this paper, we address the semi-supervised few-shot learning setting. In this setting, apart from the above episodic data, we also have access to u randomly selected samples from the classes in the episode that are not labeled. The unlabeled set can be denoted as $U = (x_i^a)_{i=0}^{N \times u}$. This leads to a setting where we have very few training samples for the classes in the episode but a good quantity of unlabeled samples. The objective of any model in this setting is to learn a good classifier for the classes in the episode using the limited supported samples and the unlabeled samples.

4. Methodology

4.1. Components

The proposed approach involves training a visual feature extractor network (M) and a semantic injection network (S). The visual feature extractor M is a simple deep neural network that, once trained, should be able to extract good features from images. The semantic injection network contains an encoder network (E_s) and a decoder network (D_s). Once trained, the semantic injection network S should be able to map features extracted by the trained visual feature extractor from an image concatenated with the semantic feature for the corresponding class to a joint embedding space where the joint feature embedding is close to the image feature prototype of the same class.

4.2. Pre-training the Visual Feature Extractor

The visual feature extractor M is first pre-trained on the train set in a regular batch-wise supervised setting. Following existing methods, we train M simultaneously on the image label classification task and the rotation prediction task (see Eq. 1), since this joint training has been shown to improve the generalization power of the network. We add an image label classification head F_c and a rotation angle classification head F_r to M for this training process.

$$L_{pt}(x_i, y_i, r_i) = L_{ce}(F_c(M(x_i)), y_i) + L_{ce}(F_r(M(x_i)), r_i) \quad (1)$$

Where, y_i and r_i refer to the image label and rotation label for image x_i , respectively. L_{ce} refers to the cross-entropy loss.

4.3. Finetuning the Visual Feature Extractor with Class-Variance Optimized Clustering

The proposed method finetunes the visual feature extractor such that it can properly cluster features of the images in the episode, assign pseudo-labels to the unlabeled samples,

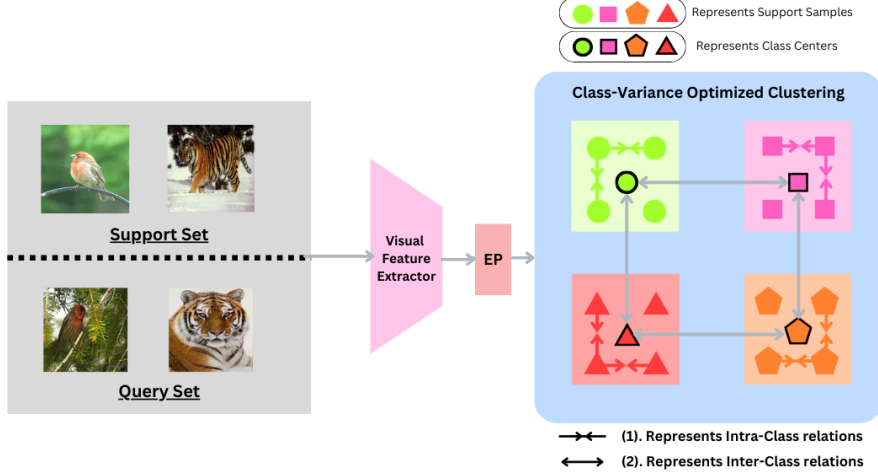


Figure 1: Finetuning the visual feature extractor. The visual feature extractor extracts features from the images in the episode, passes it through embedding propagation, and forwards the resulting features to the class-variance optimized clustering (CVOC) process. CVOC revamps the multi-factor clustering by additionally optimizing intra-class and inter-class distance losses and by utilizing the fire-fly algorithm to optimize the cluster centers .

and help in building a robust few-shot classifier. Following recent semi-supervised few-shot learning methods [22, 17], the proposed approach uses embedding propagation [22] to improve the features extracted by the visual feature extractor M . During this phase, the features extracted by M and processed using embedding propagation are passed to the class-variance optimized clustering (CVOC) process (see Fig. 1).

4.3.1 Class-Variance Optimized Clustering with Intra-Class and Inter-Class Embedding Alignment and Firefly Algorithm

CVOC revamps the multi-factor clustering method [17] using a clustering quality improvement procedure and the fire-fly algorithm [32] to get a more robust clustering of the labeled and unlabeled image features in the episode. The multi-factor clustering [17] method utilizes the class cluster centers and the support sample features as the factors representing a particular cluster. It then uses these multiple factors as a feature dictionary to represent the features of the images in the episode as a linear combination of the factors. Using the reconstruction error as the distance of an image feature from each cluster center, the multi-factor clustering method refines the cluster centers. It produces classification logits for the query images using the above distance measure from the cluster centers and finetunes the visual feature extractor using a classification loss on these predictions. Following [17] we use the classification loss based on multi-factor clustering as well as the classification loss based on label propagation [8] to train the visual feature extractor. Our proposed class-variance optimized clustering approach

improves this process by incorporating an intra-class distance loss L_{ft}^{intra} (see Eq. 2): ensuring samples are close to their respective class centers and an inter-class distance loss L_{ft}^{inter} (see Eq. 3): ensuring class centers are well-separated.

$$L_{ft}^{intra}(x_i, y_i) = d(ep(M(x_i), M(SupQry)), P(y_i)) \quad (2)$$

$$L_{ft}^{inter} = \sum_{(c_j, c_k)} -d(P(c_j), P(c_k)) \quad (3)$$

Where, y_i refer to the image label for image x_i , c_j, c_k are two different classes. $P(c_j), P(c_k)$ refers to the cluster center for the c_j^{th} and c_k^{th} class. d refers to Euclidean distance. ep refers to embedding propagation [22] that improves the embedding quality and $M(SupQry)$ refers to the features of the other images in the episode.

To further optimize the class centers, we incorporate the firefly algorithm [32] into this step. Following the firefly algorithm, each class center acts as a "firefly," whose "brightness" reflects clustering quality based on intra-class compactness and inter-class separability. In each iteration, less bright class centers are attracted toward brighter ones, guided by an attractiveness function that diminishes with distance, balancing local refinement and global exploration (see Algo 1). This process further minimizes intra-class distances and maximizes inter-class distances, leading to an optimized configuration of class centers. The result is a set of well-separated and compact clusters that improve the discriminative capability of the model on unseen data, enhancing classification performance.

Algorithm 1 Firefly Algorithm for Updating Class Centers

Require: X_{centers} : Initial class centers, S : Support set samples, S_{labels} : Labels of support set, n_{classes} : Number of classes, w_{intra} : Weight for intra-class distance, w_{inter} : Weight for inter-class distance, γ, β_0, α : Firefly algorithm parameters, n_{loops} : Number of iterations, ϵ : Threshold for penalty

Ensure: Updated X_{centers}

- 1: **Initialize Brightness:**
 - 2: **for** each class $c = 1$ to n_{classes} **do**
 - 3: Set brightness $B[c] = 0$
 - 4: **end for**
 - 5: **Main Loop:**
 - 6: **for** iteration $i = 1$ to n_{loops} **do**
 - 7: **Compute Brightness for Each Class:**
 - 8: **for** each class $c = 1$ to n_{classes} **do**
 - 9: Class Center: $\mu_c = X_{\text{centers}}[c]$
 - 10: Intra-Class Distance: $D_{\text{intra}} = \sum_{x \in S_c} \|x - \mu_c\|^2$, where S_c is the set of samples in class c
 - 11: Initialize $D_{\text{inter}} = 0$, penalty = 0
 - 12: **for** each class $k \neq c$ **do**
 - 13: $\mu_k = X_{\text{centers}}[k]$
 - 14: Distance between centers: $d = \|\mu_c - \mu_k\|$
 - 15: Update $D_{\text{inter}} += d$
 - 16: **if** $d < \epsilon$ **then**
 - 17: penalty += $(\epsilon - d)^2$
 - 18: **end if**
 - 19: **end for**
 - 20: Brightness Calculation: $B[c] = -w_{\text{intra}} \cdot D_{\text{intra}} + w_{\text{inter}} \cdot D_{\text{inter}} - \text{penalty}$
 - 21: **end for**
 - 22: **Update Class Centers Based on Brightness:**
 - 23: **for** each class $c = 1$ to n_{classes} **do**
 - 24: **for** each class $k = 1$ to n_{classes} **do**
 - 25: **if** $B[c] < B[k]$ **then**
 - 26: Distance Between Centers: $r = \|X_{\text{centers}}[c] - X_{\text{centers}}[k]\|$
 - 27: Attractiveness Calculation: $\beta = \beta_0 \cdot e^{-\gamma r^2}$
 - 28: Update Class Center:
 - 29: $X_{\text{centers}}[c] = X_{\text{centers}}[c] + \beta(X_{\text{centers}}[k] - X_{\text{centers}}[c]) + \alpha \cdot \text{randn}()$
 - 30: **end if**
 - 31: **end for**
 - 32: **end for**
 - 33: **end for**
 - 34: **Return** Updated X_{centers}
-

4.4. Training Semantic Injection Network

Once the pre-training and finetuning of the visual feature extractor (M) is finished, we train a semantic injection network (S). We extract features of images x_i from the train

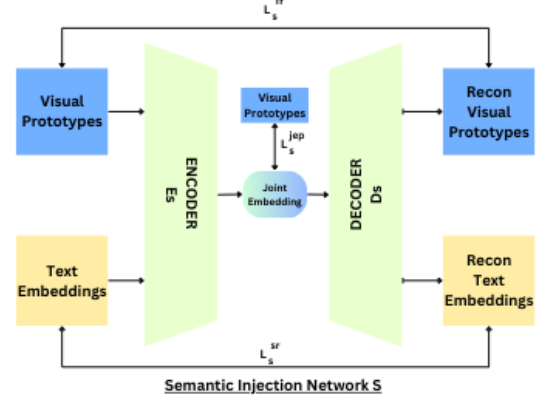


Figure 2: Training the semantic injection network. The semantic injection network’s encoder E_s takes as input the visual prototype feature and the corresponding semantic feature and produces a joint embedding. The joint embedding is mapped back to a reconstructed visual prototype feature and a reconstructed semantic feature. The training is carried out by optimizing Eq. 4.

set using the fine-tuned visual feature extractor M and embedding propagation. We obtain the class prototypes P_{c_j} by simply averaging the features from corresponding training samples from each class c_j . We also take the semantic features of the corresponding class s_{c_j} and use the encoder E_s to obtain a joint embedding $E_s(P_{c_j}, s_{c_j})$. We train S using three loss functions: joint embedding prototype loss L_s^{jep} , image feature prototype reconstruction loss L_s^{fr} , and semantic feature reconstruction loss L_s^{sr} shown in Eq. 4. The joint embedding prototype loss L_s^{jep} helps move the joint embedding closer to the image feature prototype of the same class (see Eq. 5). The image feature prototype of a class is computed by taking the mean of the features of images belonging to that class (see Eq. 6). The image feature prototype reconstruction loss L_s^{fr} is used to reduce the difference between the reconstructed prototype $P_{c_j}^r$ and the actual prototype feature P_{c_j} . Similarly, the semantic feature reconstruction loss L_s^{sr} is used to reduce the difference between the reconstructed semantic feature $s_{c_j}^r$ and the actual semantic feature s_{c_j} . The L_s^{fr} and L_s^{sr} losses force the semantic injection network to incorporate semantic information into the encoded prototype produced by E_s (see Fig. 2).

$$L_s = L_s^{jep} + L_s^{fr} + L_s^{sr} \quad (4)$$

$$L_s^{jep} = F_{L1}(E_s(P_{c_j}, s_{c_j}), P_{c_j}) \quad (5)$$

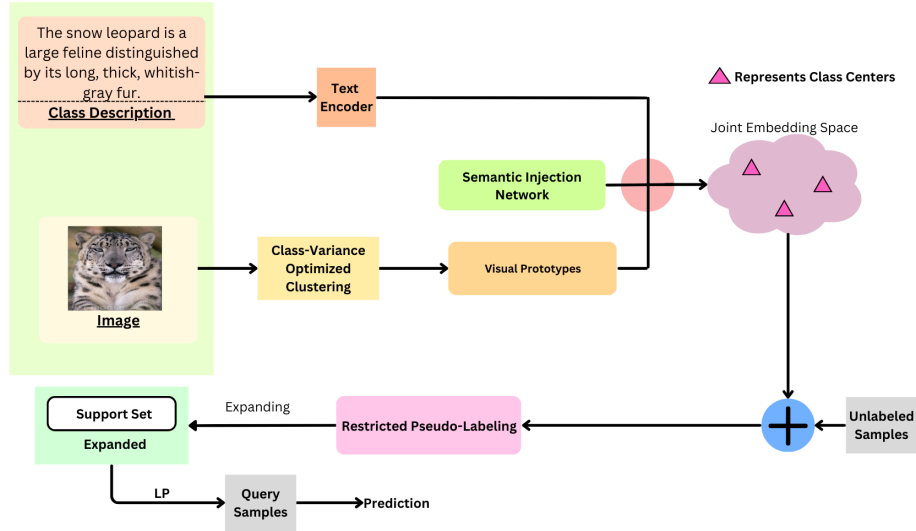


Figure 3: Evaluation using semantic injection and restricted pseudo-labeling. Class-variance optimized clustering is used to obtain the visual prototype features per class, which are refined using the semantic injection network. Restricted pseudo-labeling of the unlabeled samples in the episode helps to expand the support set. Label propagation [8] (LP) is used to predict the class for the query samples using the expanded support set.

$$P_{c_j} = \frac{1}{N_{c_j}} \sum_{(x_i, y_i) \in D_{tr}} \mathbb{1}(y_i == c_j) ep(M(x_i), M(SupQry)) \quad (6)$$

$$P_{c_j}^r, s_{c_j}^r = D_s(E_s(P_{c_j}, s_{c_j})) \quad (7)$$

$$L_s^{fr} = F_{L1}(P_{c_j}^r, P_{c_j}) \quad (8)$$

$$L_s^{sr} = F_{L1}(s_{c_j}^r, s_{c_j}) \quad (9)$$

Where, F_{L1} refers to an L1-loss, P_{c_j} refers to the prototype for the c_j class, N_{c_j} refers to the number of labeled samples belonging to class c_j .

4.5. Evaluation Process with Semantic Injection and Restricted Pseudo-Labeling

Once the visual feature extractor has completed the pre-training and fine-tuning steps, we evaluate it on N-way K-shot episodes from the test set. These episodes contain a few labeled support examples from the few-shot classes and also some unlabeled samples from the classes in the episode.

The proposed method uses multi-factor clustering with the fire-fly algorithm to obtain the cluster centers. We then perform **semantic injection** by concatenating each

cluster center with the corresponding class semantic feature and using the encoder E_s of the trained semantic injection network to produce a joint embedding representing the cluster center incorporated with semantic information. We obtain the refined cluster center by combining the original cluster center and the output of the semantic injection network encoder using a hyper-parameter s as: $P^{ref}(y_i) = s \times P(y_i) + (1 - s) \times E_s(P(y_i), s_{y_i})$. We use the refined cluster centers $P^{ref}(y_i)$ to obtain classification logits for the unlabeled samples. The classification logits are obtained using the distance of the sample from all the cluster centers.

While analyzing the code [16] for cluster-FSL [17], we observed that while running, it was effectively selecting almost all of the unlabeled samples for pseudo-labeling. Different from cluster-FSL [17], we do not assign pseudo-labels to all the unlabeled samples. Instead, we perform a **restricted pseudo-labeling process** to only perform pseudo-labeling for the top $k\%$ samples for which the predictions have a relatively lower entropy. This involves first obtaining the entropy of the classification logits obtained for the unlabeled samples. The unlabeled samples with prediction entropy below a particular threshold, are only provided pseudo-labels. The threshold is decided based on the hyper-parameter k , which refers to the top $k\%$ samples with the lowest prediction entropy that are selected for pseudo-labeling. The pseudo-labels are obtained for the chosen unlabeled samples by considering the class with the highest logit value in the

classification logits of these unlabeled samples. The rest of the unlabeled samples are not used. This increases the size of the support set for the current episode. Similar to existing methods, we then predict the labels of the query samples using label propagation [8] from the expanded support set (see Fig. 3).

5. Experimental Results

5.1. Implementation Details

The semi-supervised few-shot learning methods are evaluated on the miniImageNet [29], tieredImageNet [21] and CUB [4] datasets. Due to limitation of space, please refer to the supplementary material for further details on the datasets used, the implementation details and the compared methods.

5.2. Results

We conducted experiments under 5-way 1-shot and 5-way 5-shot scenarios on WRN-28-10 and ResNet-12 backbones, obtaining results on miniImageNet, tieredImageNet, and CUB-200-2011 datasets, as detailed in Tables 1, 2, and 3. For miniImageNet, our CVOCSemRPL model outperformed cluster-FSL [17], achieving a 6.7% and 1.4% improvement in 1-shot and 5-shot settings with ResNet-12, and a 3.31% and 1.87% improvement with WRN-28-10. On the tieredImageNet dataset (Table 2), CVOCSemRPL outperforms the closest method by margins of 1.66% and 1.19% for 1-shot and 5-shot cases with ResNet-12, and by a margin of 3.32% for 1-shot and 1.35% for 5-shot settings with WRN-28-10.

On the CUB-200-2011 dataset (Table 3), CVOCSemRPL outperformed EPNet [22] and cluster-FSL [17], though with lower improvement gains. This limited gain is likely due to the homogeneity of the bird-only classes in CUB-200-2011, leading to reduced discriminative power since the semantic centers are closely aligned (e.g., all birds possess common features such as wings, beaks, and legs), contrasting with the broader class diversity in ImageNet [23] datasets like miniImageNet and tieredImageNet.

6. Ablation Experiments

6.1. Hyper-parameter selection

In this section, we discuss the results of the hyper-parameter tuning carried out for our approach. The experiments are carried out on the miniImageNet dataset using the ResNet12 network. Fig. 7 indicates that $k=0.8$ is the most suitable value, i.e., when the threshold for entropy is set according to allowing the 80% of the unlabeled samples that have the lowest prediction entropy, to be provided with a pseudo-label. Fig. 8 indicates that $s=0.9$ is the most suitable value for combining the visual prototype with the semantic information injected prototype.

Methods	5-way	
	1-shot	5-shot
<i>ResNet-12</i>		
TADAM	58.50±0.30%	76.70±0.30%
MTL	61.20±1.80%	75.50±0.80%
MetaOpt-SVM	62.64±0.61%	78.60±0.46%
CAN	67.19±0.55%	80.64±0.35%
LST	70.10±1.90%	78.70±0.80%
EPNet	66.50±0.89%	81.06±0.60%
TPN	59.46%	75.65%
PLAIN	74.38±2.06%	82.02±1.08%
EPNet-SSL	75.36±1.01%	84.07±0.60%
cluster-FSL	77.81±0.81%	85.55±0.41%
CVOCSemRPL (ours)	84.51±0.54%	86.95±0.39%
<i>WRN-28-10</i>		
Soft K-Means	50.09±0.45%	64.59±0.28%
Soft K-Means+Cluster	49.03±0.24%	63.08±0.18%
Masked Soft K-Means	50.41±0.31%	64.39±0.24%
LEO	61.76±0.08%	77.59±0.12%
wDAE-GNN	62.96±0.62%	78.85±0.10%
EPNet	80.74±0.85%	84.34±0.53%
TransMatch	62.93±1.11%	82.24±0.59%
ICI	71.41%	81.12%
EPNet-SSL	79.22±0.92%	88.05±0.51%
PTN	81.57±0.94%	87.17±0.58%
cluster-FSL	82.63±0.79%	89.16±0.35%
CVOCSemRPL (ours)	85.94±0.58%	91.03±0.47%

Table 1: Classification accuracy (%) on the miniImageNet dataset with different FSL settings and backbone architecture.

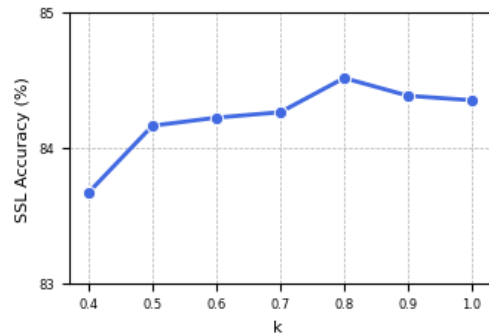


Figure 4: Effect of $k \times 100\%$ Restricted Pseudo Labeling on semi-FSL Accuracy on the miniImageNet dataset 5w1s using ResNet12.

Methods	5-way	
	1-shot	5-shot
<i>ResNet-12</i>		
MetaOpt-SVM	65.99±0.72%	81.56±0.53%
CAN	73.21±0.58%	84.93±0.38%
LST	77.70±1.60%	85.20±0.80%
EPNet	76.53±0.83%	84.80±0.98%
PLML-EP	79.62%	86.69%
PLAIN	82.91±2.09%	89.28±1.25%
EPNet-SSL	81.79±0.97%	88.45±0.61%
cluster-FSL	83.89±0.81%	89.94±0.46%
CVOCSemRPL (ours)	85.55±0.98%	91.13±0.54%
<i>WRN-28-10</i>		
Soft K-Means	51.52±0.36%	70.25±0.31%
Soft K-Means+Cluster	50.33±0.24%	71.03±0.22%
Masked Soft K-Means	52.39±0.44%	69.46±0.24%
LEO	61.76±0.08%	78.43±0.12%
wDAE-GNN	68.16±0.46%	82.96±0.51%
EPNet	78.50±0.31%	88.90±0.57%
ICI	85.44%	89.12%
EPNet-SSL	83.68±0.69%	89.00±0.52%
PTN	84.70±1.54%	89.14±0.73%
cluster-FSL	85.74±0.76%	90.18±0.43%
CVOCSemRPL (ours)	89.06±0.58%	91.53±0.39%

Table 2: Classification accuracy (%) on the tieredImageNet dataset with different FSL settings and backbone architecture.

Methods	5-way	
	1-shot	5-shot
<i>ResNet-12</i>		
EPNet	82.85±0.81%	91.32±0.41%
cluster-FSL	87.36±0.71%	92.17±0.31%
CVOCSemRPL (ours)	88.37±0.73%	93.03±0.15%
<i>WRN-28-10</i>		
ICI	91.11%	92.98%
EPNet	87.75±0.70%	94.03±0.33%
cluster-FSL	91.80±0.58%	95.07±0.23%
CVOCSemRPL (ours)	92.66±0.59%	95.87±0.24%

Table 3: Classification accuracy (%) on the CUB dataset with different FSL settings and backbone architecture.

6.2. Contribution of the Components

In this section, we perform ablation experiments to analyze the contributions of various components of our approach

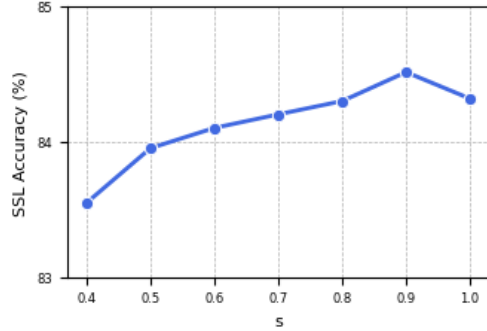


Figure 5: Effect of value of s which determines final refined prototype for clustering in the testing phase on the miniImageNet dataset 5w1s using ResNet12.

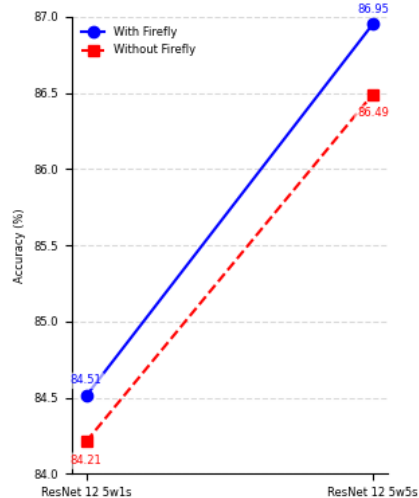


Figure 6: Effect of firefly optimization on the miniImageNet dataset 5w1s and 5w5s using ResNet12.

Intra-Inter Class loss	Semantic Injection	5w1s	5w5s
×	×	78.31 ± 0.79%	85.75 ± 0.41%
✓	×	80.29 ± 0.54%	85.91 ± 0.79%
×	✓	82.53 ± 0.52%	86.45 ± 0.41%
✓	✓	84.51 ± 0.54%	86.95% ± 0.39%

Table 4: Impact of the intra-inter class distance loss in fine-tuning and semantic injection in the testing phase on the miniImageNet dataset 5w5s and 5w1s using ResNet12.

using the miniImageNet dataset and ResNet12 architecture. Specifically, we study the effect of our firefly-based class center update algorithm, semantic injection, and the intra-inter class loss. The results in 4 indicate that removing the semantic injection or intra-inter class loss significantly

degrades the performance of our method. Similarly, Fig. 6 indicates the usefulness of the firefly algorithm.

7. Conclusion

In this work, we proposed a novel approach that improves clustering based pseudo-labeling in semi-supervised few-shot learning using intra/inter class distance losses, firefly algorithm and semantic features. We have experimentally shown that the proposed approach significantly outperforms the recent methods.

References

- [1] Xingping Dong, Tianran Ouyang, Shengcai Liao, Bo Du, and Ling Shao. Pseudo-labeling based practical semi-supervised meta-training for few-shot learning. *IEEE Transactions on Image Processing*, 2024.
- [2] Chelsea Finn, Pieter Abbeel, and Sergey Levine. Model-agnostic meta-learning for fast adaptation of deep networks. In *International conference on machine learning*, pages 1126–1135. PMLR, 2017.
- [3] Spyros Gidaris and Nikos Komodakis. Generating classification weights with gnn denoising autoencoders for few-shot learning. In *Proceedings of the IEEE/CVF conference on computer vision and pattern recognition*, pages 21–30, 2019.
- [4] Nathan Hilliard, Lawrence Phillips, Scott Howland, Artëm Yankov, Courtney D Corley, and Nathan O Hodas. Few-shot learning with metric-agnostic conditional embeddings. *arXiv preprint arXiv:1802.04376*, 2018.
- [5] Ruibing Hou, Hong Chang, Bingpeng Ma, Shiguang Shan, and Xilin Chen. Cross attention network for few-shot classification. *Advances in neural information processing systems*, 32, 2019.
- [6] Huaxi Huang, Junjie Zhang, Jian Zhang, Qiang Wu, and Chang Xu. Ptn: A poisson transfer network for semi-supervised few-shot learning. In *Proceedings of the AAAI Conference on Artificial Intelligence*, volume 35, pages 1602–1609, 2021.
- [7] Kai Huang, Jie Geng, Wen Jiang, Xinyang Deng, and Zhe Xu. Pseudo-loss confidence metric for semi-supervised few-shot learning. In *Proceedings of the IEEE/CVF international conference on computer vision*, pages 8671–8680, 2021.
- [8] Ahmet Iscen, Giorgos Tolias, Yannis Avrithis, and Ondrej Chum. Label propagation for deep semi-supervised learning. In *Proceedings of the IEEE/CVF conference on computer vision and pattern recognition*, pages 5070–5079, 2019.
- [9] Zhong Ji, Xingliang Chai, Yunlong Yu, and Zhongfei Zhang. Reweighting and information-guidance networks for few-shot learning. *Neurocomputing*, 423:13–23, 2021.
- [10] Jędrzej Kozerawski and Matthew Turk. Clear: Cumulative learning for one-shot one-class image recognition. In *Proceedings of the IEEE Conference on Computer Vision and Pattern Recognition*, pages 3446–3455, 2018.
- [11] Michalis Lazarou, Tania Stathaki, and Yannis Avrithis. Iterative label cleaning for transductive and semi-supervised few-shot learning. In *Proceedings of the IEEE/CVF international conference on computer vision*, pages 8751–8760, 2021.
- [12] Kwonjoon Lee, Subhansu Maji, Avinash Ravichandran, and Stefano Soatto. Meta-learning with differentiable convex optimization. In *Proceedings of the IEEE/CVF conference on computer vision and pattern recognition*, pages 10657–10665, 2019.
- [13] Pan Li, Guile Wu, Shaogang Gong, and Xu Lan. Semi-supervised few-shot learning with pseudo label refinement. In *2021 IEEE International Conference on Multimedia and Expo (ICME)*, pages 1–6. IEEE, 2021.
- [14] Xinzhe Li, Qianru Sun, Yaoyao Liu, Qin Zhou, Shibao Zheng, Tat-Seng Chua, and Bernt Schiele. Learning to self-train for semi-supervised few-shot classification. *Advances in neural information processing systems*, 32, 2019.
- [15] Zhenguo Li, Fengwei Zhou, Fei Chen, and Hang Li. Meta-sgd: Learning to learn quickly for few-shot learning. *arXiv preprint arXiv:1707.09835*, 2017.
- [16] Jie Ling, Lei Liao, Meng Yang, and Jia Shuai. Code for Semi-Supervised Few-shot Learning via Multi-Factor Clustering.
- [17] Jie Ling, Lei Liao, Meng Yang, and Jia Shuai. Semi-supervised few-shot learning via multi-factor clustering. In *Proceedings of the IEEE/CVF Conference on Computer Vision and Pattern Recognition*, pages 14564–14573, 2022.
- [18] Yanbin Liu, Juho Lee, Minseop Park, Saehoon Kim, Eunho Yang, Sung Ju Hwang, and Yi Yang. Learning to propagate labels: Transductive propagation network for few-shot learning. *arXiv preprint arXiv:1805.10002*, 2018.
- [19] Boris Oreshkin, Pau Rodríguez López, and Alexandre Lacoste. Tadam: Task dependent adaptive metric for improved few-shot learning. *Advances in neural information processing systems*, 31, 2018.
- [20] Sachin Ravi and Hugo Larochelle. Optimization as a model for few-shot learning. In *International conference on learning representations*, 2017.
- [21] Mengye Ren, Eleni Triantafillou, Sachin Ravi, Jake Snell, Kevin Swersky, Joshua B Tenenbaum, Hugo Larochelle, and Richard S Zemel. Meta-learning for semi-supervised few-shot classification. *arXiv preprint arXiv:1803.00676*, 2018.
- [22] Pau Rodríguez, Issam Laradji, Alexandre Drouin, and Alexandre Lacoste. Embedding propagation: Smoother manifold for few-shot classification. In *Computer Vision—ECCV 2020: 16th European Conference, Glasgow, UK, August 23–28, 2020, Proceedings, Part XXVI 16*, pages 121–138. Springer, 2020.
- [23] Olga Russakovsky, Jia Deng, Hao Su, Jonathan Krause, Sanjeev Satheesh, Sean Ma, Zhiheng Huang, Andrej Karpathy, Aditya Khosla, Michael Bernstein, et al. Imagenet large scale visual recognition challenge. *International journal of computer vision*, 115:211–252, 2015.
- [24] Andrei A Rusu, Dushyant Rao, Jakub Sygnowski, Oriol Vinyals, Razvan Pascanu, Simon Osindero, and Raia Hadsell. Meta-learning with latent embedding optimization. *arXiv preprint arXiv:1807.05960*, 2018.
- [25] Jake Snell, Kevin Swersky, and Richard Zemel. Prototypical networks for few-shot learning. *Advances in neural information processing systems*, 30, 2017.
- [26] Heda Song, Mercedes Torres Torres, Ender Özcan, and Isaac Triguero. L2ae-d: Learning to aggregate embeddings for

few-shot learning with meta-level dropout. *Neurocomputing*, 442:200–208, 2021.

- [27] Qianru Sun, Yaoyao Liu, Tat-Seng Chua, and Bernt Schiele. Meta-transfer learning for few-shot learning. In *Proceedings of the IEEE/CVF conference on computer vision and pattern recognition*, pages 403–412, 2019.
- [28] Flood Sung, Yongxin Yang, Li Zhang, Tao Xiang, Philip HS Torr, and Timothy M Hospedales. Learning to compare: Relation network for few-shot learning. In *Proceedings of the IEEE conference on computer vision and pattern recognition*, pages 1199–1208, 2018.
- [29] Oriol Vinyals, Charles Blundell, Timothy Lillicrap, Daan Wierstra, et al. Matching networks for one shot learning. *Advances in neural information processing systems*, 29, 2016.
- [30] Yikai Wang, Chengming Xu, Chen Liu, Li Zhang, and Yanwei Fu. Instance credibility inference for few-shot learning. In *Proceedings of the IEEE/CVF conference on computer vision and pattern recognition*, pages 12836–12845, 2020.
- [31] Yu Wu, Yutian Lin, Xuanyi Dong, Yan Yan, Wanli Ouyang, and Yi Yang. Exploit the unknown gradually: One-shot video-based person re-identification by stepwise learning. In *Proceedings of the IEEE conference on computer vision and pattern recognition*, pages 5177–5186, 2018.
- [32] Xin-She Yang and Xingshi He. Firefly algorithm: recent advances and applications. *International journal of swarm intelligence*, 1(1):36–50, 2013.
- [33] Donghyun Yoo, Haoqi Fan, Vishnu Boddeti, and Kris Kitani. Efficient k-shot learning with regularized deep networks. In *Proceedings of the AAAI conference on artificial intelligence*, volume 32, 2018.
- [34] Zhongjie Yu, Lin Chen, Zhongwei Cheng, and Jiebo Luo. Transmatch: A transfer-learning scheme for semi-supervised few-shot learning. In *Proceedings of the IEEE/CVF conference on computer vision and pattern recognition*, pages 12856–12864, 2020.

8. Supplementary

8.1. Experimental Settings

8.1.1 Datasets

The *miniImageNet* dataset [29] is a subset of ImageNet [23], consisting of 60,000 images, from 64 training classes, 16 validation classes, and 20 testing classes. The *tieredImageNet* dataset [21], is another subset of ImageNet [23] that is designed specifically for few-shot learning applications. This dataset of 779,165 images, includes a hierarchical structure with 34 superclasses divided into 608 fine-grained categories, encompassing a wide range of natural and artificial objects, animal species, and other general image classes. The dataset is partitioned into 20 training superclasses (covering 351 classes), 6 validation superclasses (97 classes), and 8 test superclasses (160 classes). The CUB dataset [4], derived from the fine-grained Caltech-UCSD Birds-200-2011 dataset [43], contains 200 classes representing 11,788 images of birds.

This dataset is partitioned into 100,50 and 50 classes for the base, validation, and novel class split.

8.1.2 Pretraining

In the pre-training phase of the proposed approach, the network is trained for 150 epochs on the base classes using batches of 128 images. The output feature dimensions are 640 for the WRN-28-10 architecture and 512 for ResNet-12.

8.1.3 Finetuning

In the fine-tuning phase, the model refines the cluster centers through iterative optimization. Initially, class centers are computed from the support set. Then, the model adjusts these centers by minimizing the intra-class variance (ensuring samples within a class are close) and maximizing the inter-class distance (separating classes). The model further optimizes the embeddings by reducing the reconstruction error between support and query samples. The process continues for a set number of iterations until convergence, improving the overall clustering quality.

Additionally, the Semantic Injection Network is trained using the trained weights from CVOCSemRPL, enhancing the semantic alignment between visual embeddings and reconstructed prototypes. This setup is crucial for optimizing the model’s performance in handling both visual and textual data in a semi-supervised learning framework.

8.1.4 Testing

For testing, a hybrid approach is employed. The clustering process labels the top-k% samples with lower entropy as support examples, while the remaining unlabeled samples are assigned labels via embedding propagation. The pre-trained semantic alignment network helps align text and visual embeddings, and the reconstructed cluster centers guide label assignment.

8.1.5 Compared Methods

The baseline models for our comparative experiments include cluster-FSL [17], PLML+EP [1], EPNet [22], ICI [30], and state-of-the-art few-shot learning methods such as TADAM [19], MTL [27], MetaOpt-SVM [12], CAN [5], LST [28], and LEO [24]. Semi-supervised approaches like TPN [18], TransMatch [34], and PLAIN [13], as well as graph-based methods such as wDAE-GNN [3], were also tested. Additionally, we compared our model with PTN [6] and clustering approaches by Ren et al. [21], including Soft K-Means, Soft K-Means+Cluster, and Masked Soft K-Means. In contrast to cluster-FSL, which uses quantitative analysis to evaluate model classification accuracy, our

method leverages semantic context, inter-class and intra-class variance, and unlabeled samples with low prediction entropy for improved testing accuracy.

8.2. Ablation Experiments

8.2.1 Hyper-parameter selection

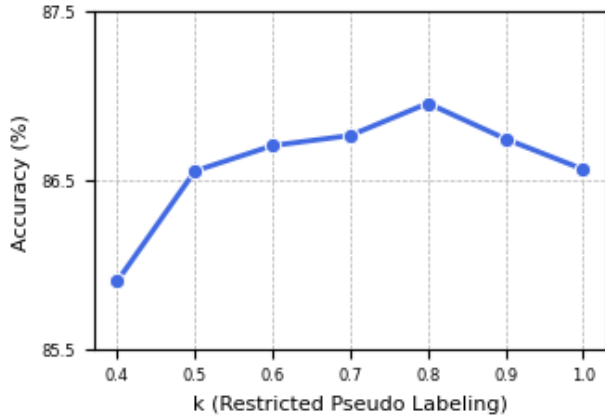


Figure 7: Effect of $k \times 100\%$ Restricted Pseudo Labeling on semi-FSL Accuracy on the *miniImageNet* dataset 5w5s using ResNet12.

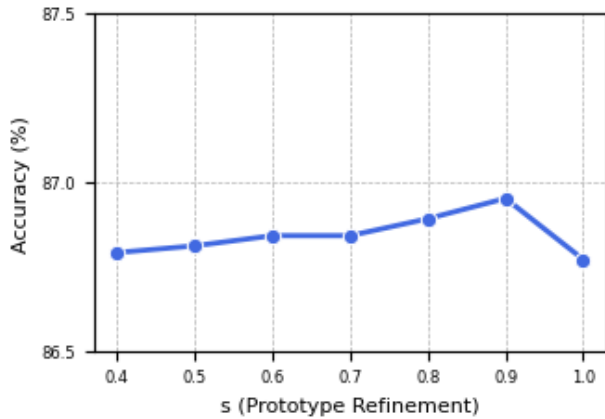


Figure 8: Effect of the value of s which determines final refined prototype for clustering in the testing phase on the *miniImageNet* dataset 5w5s using ResNet12.

In this section, we discuss the results of the hyper-parameter tuning carried out for our approach. The experiments are carried out on the *miniImageNet* dataset using the ResNet12 network. Fig. 7 indicates that $k=0.8$ is the most suitable value, i.e., when the threshold for entropy is set according to allowing the 80% of the unlabeled samples that have the lowest prediction entropy, to be provided with a

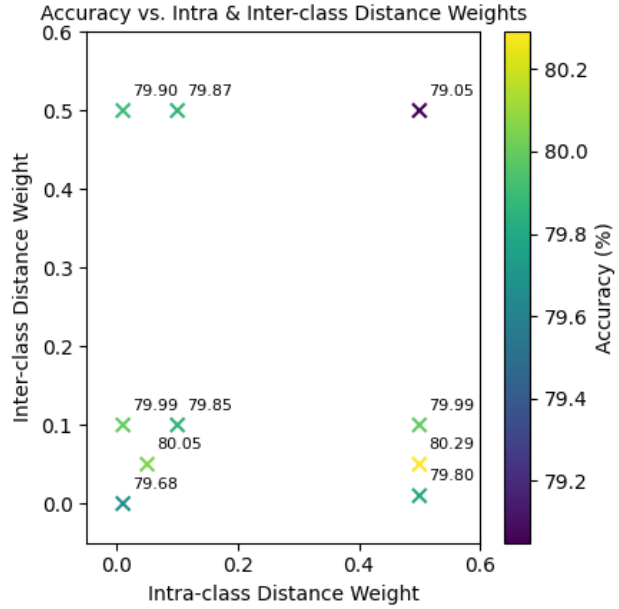


Figure 9: Effect of intra and inter-class distance weights during fine-tuning on the *miniImageNet* dataset 5w1s using ResNet12 **without semantic injection** during testing.

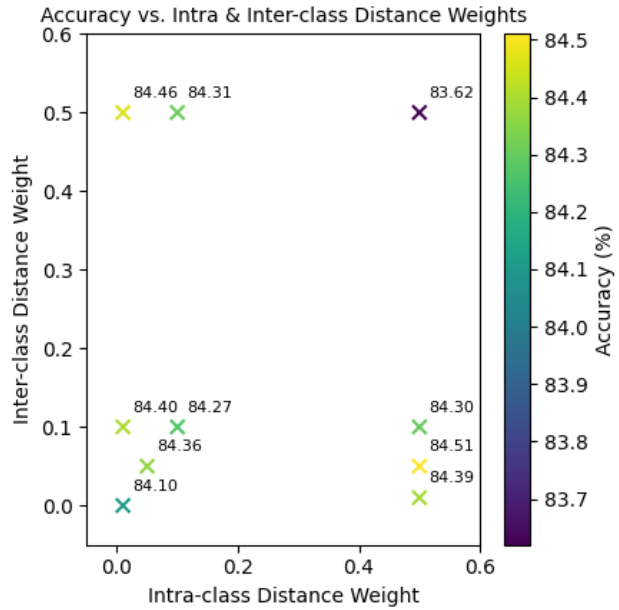


Figure 10: Effect of intra and inter-class distance weights during finetuning on the *miniImageNet* dataset 5w1s using ResNet12 **with semantic injection** during testing.

pseudo-label. Fig. 8 indicates that $s = 0.9$ is the most suitable value for combining the visual prototype with the semantic information injected prototype.

γ	Average Semi-FSL Accuracy (%)
0.5	84.03
1.0	84.21
2.0	84.29
5.0	83.94

Table 5: Analysis of the effect of γ on the *miniImageNet* dataset 5w1s using ResNet12.

Fig. 9 & Fig. 10 further examine the effect of intra-class and inter-class distance weights during the fine-tuning phase. Fig. 9 plot shows the results **without semantic injection** during testing. It is observed that the highest accuracy is achieved for an intra-class distance weight of 0.5 and an inter-class distance weight of 0.05. Fig. 10 plot illustrates the results **with semantic injection** during testing. The best accuracy is still obtained for an intra-class weight of 0.5 and an inter-class weight of 0.05.

8.3. Hyperparameter Analysis of the Firefly Algorithm

In this section, we present a comprehensive hyperparameter analysis of the firefly algorithm (FA) applied to the ResNet12 architecture on the *miniImageNet* dataset under the 5-way 1-shot setting. The key hyperparameters of the FA are the light absorption coefficient (γ), the maximum attractiveness (β_0), the randomization parameter (α), and the inter-class distance penalty threshold (ϵ).

8.3.1 Effect of Light Absorption Coefficient (γ)

The light absorption coefficient γ controls how quickly the attractiveness between fireflies decreases with distance. A higher γ value causes the attractiveness to diminish more rapidly, making each firefly primarily influenced by nearby brighter fireflies. Adjusting γ balances exploration and exploitation: increasing γ promotes local search around current solutions while decreasing it encourages broader exploration of the solution space.

We evaluated the effect of varying γ on the average semi-supervised few-shot learning (Semi-FSL) accuracy. The results are presented in Table 5. As observed, the accuracy slightly improves as γ increases from 0.5 to 2.0, with the highest accuracy of 84.29% achieved at $\gamma = 2.0$. However, further increasing γ to 5.0 leads to a decrease in accuracy.

8.3.2 Effect of Maximum Attractiveness (β_0)

The parameter β_0 represents the maximum attractiveness between fireflies when they are at zero distance from each other. It scales the strength of the attraction forces, effectively controlling the step size towards brighter fireflies. A larger β_0

β_0	Average Semi-FSL Accuracy (%)
0.5	83.90
1.0	84.26
2.0	83.88

Table 6: Analysis of the effect of β_0 on the *miniImageNet* dataset 5w1s using ResNet12.

α	Average Semi-FSL Accuracy (%)
0.5	83.99
0.1	84.23
0.05	84.17

Table 7: Analysis of the effect of α on the *miniImageNet* dataset 5w1s using ResNet12.

increases the influence of brighter fireflies on others, potentially accelerating convergence to optimal solutions. However, too high a value may lead to premature convergence, reducing the algorithm’s ability to explore diverse solutions.

Table 6 shows the effect of varying β_0 . The highest accuracy of 84.26% is achieved at $\beta_0 = 1.0$. Increasing β_0 beyond this point does not improve performance, indicating that an optimal balance between exploration and exploitation is achieved at $\beta_0 = 1.0$.

8.3.3 Effect of Randomization Parameter (α)

The randomization parameter α determines the magnitude of stochastic perturbations in the fireflies’ movements. It introduces randomness to avoid local optima and maintain diversity in the population. A higher α increases the randomness, enhancing exploration capabilities but potentially slowing down convergence. Conversely, a lower α reduces randomness, promoting the exploitation of known good solutions but risking entrapment in local minima.

As shown in Table 7, an α value of 0.1 yields the highest accuracy of 84.23%. Both increasing and decreasing α from this value result in a slight decrease in performance, indicating that $\alpha = 0.1$ provides an optimal balance.

8.3.4 Effect of Inter-Class Distance Penalty Threshold (ϵ)

The parameter ϵ sets a threshold for penalizing inter-class distances that are below a certain value, effectively enforcing a minimum separation between class centers. If the distance between class centers is less than ϵ , a penalty is applied to encourage greater separation. Adjusting ϵ impacts the balance between inter-class discrimination and intra-class compactness: a larger ϵ enforces a stricter separation between classes,

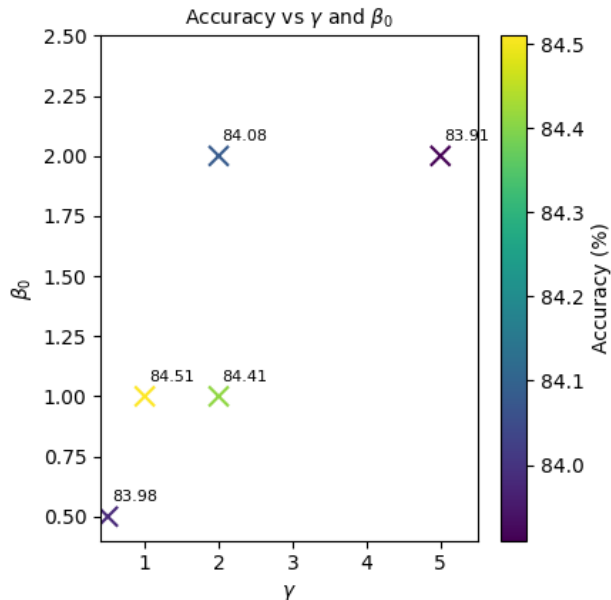


Figure 11: Effect of various hyperparameters of the **firefly algorithm** on the *miniImageNet* dataset 5w1s using ResNet12 with semantic injection during testing. α and ϵ are kept at 0.1 and 2.0, respectively.

ϵ	Average Semi-FSL Accuracy (%)
1.0	83.96
2.0	84.20
5.0	83.98

Table 8: Analysis of the effect of ϵ on the *miniImageNet* dataset 5w1s using ResNet12.

which can improve classification performance but may also affect the compactness of clusters within each class.

From Table 8, we observe that setting $\epsilon = 2.0$ results in the highest accuracy of 84.20%. This suggests that enforcing a moderate minimum separation between class centers enhances classification performance.

8.3.5 Combined Effect of Hyperparameters

To further illustrate the impact of the FA hyperparameters, we present Fig. 11, which shows the effect of varying γ and β_0 on the accuracy, with α and ϵ kept constant at 0.1 and 2.0, respectively. The figure demonstrates that the optimal performance is achieved when $\gamma = 2.0$ and $\beta_0 = 1.0$, corroborating the findings from the individual analyses.